PHYSICAL REVIEW A VOLUME 23, NUMBER 2 FEBRUARY 1981

Single-electron-capture cross section for medium- and high-velocity, highly charged ions colliding with atoms

H. Knudsen, H. K. Haugen, and P. Hvelplund
Institute of Physics, University of Aarhus, DK-8000 Aarhus C, Denmark
(Received 6 June 1980)

Experimental cross sections for single-electron capture for medium- to high-energy, highly charged oxygen and gold ions colliding with helium atoms are presented. Simple estimates based on the classical cross sections introduced by Bohr and Lindhard for multiply charged ions are shown to lead to good first approximations of the absolute magnitude of the cross sections for any target atom. Furthermore, these estimates suggest a universal scaling of the capture cross sections with ion and target-atom parameters. The experimental results of this work as well as those obtained by other groups are shown to be in accordance with the suggested scaling laws, which are also supported by the results of the few more-refined theoretical treatments that have been published.

I. INTRODUCTION

In the present paper, we shall consider the charge-exchange process,

$$A^{q+} + B \rightarrow A^{(q-1)+} + B^{+}, \tag{1}$$

in which an energetic ion A of charge $+qe$ during a collision with a neutral atom B picks up one of the atomic electrons, thereby emerging with a charge $+(q-1)e$.

Electron capture was first observed by Henderson[1] in the early 1920's. Since then, there has been a continuous interest in these processes, partly due to the fact that in single collisions between ions and atoms, the electron-capture exit channel is often associated with a large cross section, thus making the process important for the understanding of such collisions, and partly due to the influence of charge exchange on the slowing down of atomic particles passing through matter.

However, the study of electron-capture processes has been hampered by the absence of an adequate general theoretical treatment. This problem stems from the fact that the process involves a three-body interaction, which is difficult to treat theoretically starting from basic principles.

Recently, there has been a substantial increase in the activity in this field as regards theoretical as well as experimental investigations. This renewed interest stems from both that electron-capture processes have been found to be crucial for the performance of thermonuclear-fusion devices,[2] and from the importance of such processes in astrophysics.[3] For both of these fields, a large number of important reactions exist, in which the capturing ion is highly charged and for which the relative velocity of the collision partners is $\gtrsim v_0$, the first Bohr-orbital velocity.

This study reports on measurements of the single-electron-capture cross section for MeV oxygen and gold ions colliding with helium atoms. Furthermore, simple theoretical estimates of the capture cross sections based on the model of Bohr and Lindhard[4] are presented. These estimates lead to quantitative results as well as to universal scaling laws, and a comparison with the present experimental data and data obtained by other investigators is shown to support the applicability of the theoretical model.

II. EXPERIMENTAL

For the present experiments, a monoenergetic beam of MeV oxygen or gold ions is obtained from the Aarhus University EN tandem accelerator and charge and energy analyzed in an analyzing magnet. It then enters the setup shown in Fig. 1 where, depending on whether low, medium, or high charges are desired, the beam particles are passed directly to the switching magnet, stripped by a low-pressure gas between the analyzing and switching magnet, or passed through a thin carbon foil, from which the ions emerge with a broad range of high charges. A beam component having the desired charge is then selected in the switching magnet and passed through an ~8m-long beam line, in which the pressure is lower than 1×10^{-6} torr. Although the pressure is rather low, a small part of the ions experience charge-changing collisions in the beam line. To remove such ions, the beam is passed through a set of electrostatic deflection plates, from which the ions emerge into a region where the background pressure is below 5×10^{-7} torr. Here the beam passes through a differentially pumped gas cell, and after having interacted with the target gas, the beam particles are charge analyzed by a second set of electrostatic deflection plates. Finally, the charge components are detected by a movable, position-

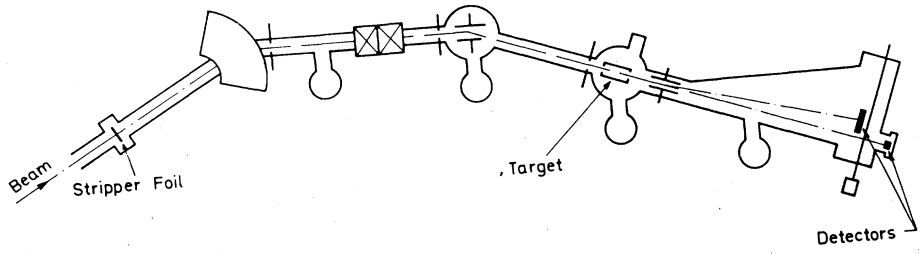

FIG. 1. Schematic drawing of the experimental setup.

sensitive solid-state detector, which, for the target pressures used, collects all particles that pass through the gas cell. The target gas was 99.99% pure helium and its pressure p was measured with a Pirani gauge calibrated against a membrane manometer.

The experimental single-capture cross section σ_C was obtained from the expression

$$\sigma_C = \lim_{p\to 0}\left(\frac{N_{q-1} - N^0_{q-1}}{N_{\text{tot}} p L\, 3.29\times 10^{16}}\right) \text{cm}^2 , \qquad (2)$$

where p is measured in torr, L is the target-gas-cell length (=22.0 cm) corrected +0.5% for pressure variations outside the entrance and exit apertures, N_{tot} is the total number of beam particles, N_{q-1} is the number of particles recorded as having charge $q-1$, and N^0_{q-1} is the small amount (always less than 1% of N_{tot}) of particles of charge $q-1$ recorded with no gas in the target-gas cell. The target pressure was always kept low enough (~1 mtorr) to ensure a linear extrapolation of Eq. (2) to zero pressure.

The main source of error on the relative values of σ_C stems from the extrapolation. For cases where the capture cross section is low (low q), the linear part of the extrapolation curve extended to rather high pressures, and σ_C was found to within 2%. For high q, where σ_C is large, the curve was linear only at very low pressures, and consequently, relative uncertainties up to 10% are associated with the corresponding measured cross sections. The calibration of the Pirani gauge against a membrane manometer introduced a further uncertainty of 5% on the absolute magnitude of σ_C.

The experimental results for the single-electron-capture cross section for 3.3-MeV Au^{q+} ($q=2$–8), 20-MeV Au^{q+} ($q=6$–24), 2.0-MeV O^{q+} ($q=1$–6), and 16-MeV O^{q+} ($q=3$–8) on helium plotted versus the ionic charge are shown in Fig. 2. The cross sections increase with increasing charge and, for ion velocities greater than v_0, decrease rapidly with increasing ion velocity. The curves also shown in Fig. 2 are the results of theoretical estimates, which will be discussed in the following section.

To ensure that the measured cross sections correspond to a well-defined collision process, it is necessary to know not only the charge state of the incoming ions but also their state of excitation. If the beam contained a non-negligible fraction of metastable ions, this might alter the capture cross section in an unpredictable way as

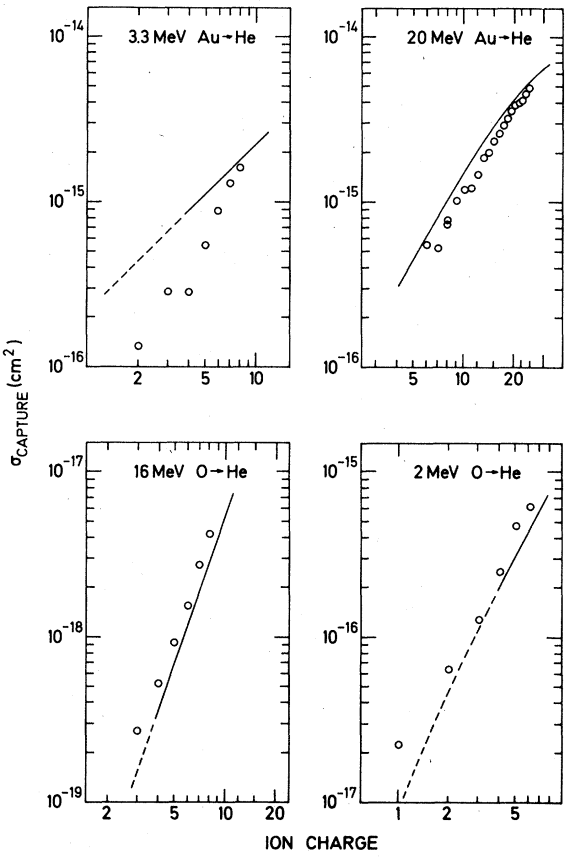

FIG. 2. The experimental single-capture cross section for O and Au ions colliding with He atoms (this work). The data are compared to the theoretical estimate [Eq. (17)] where a value of $\alpha = 0.40$ has been used.

compared to the situation where the ions were all in the ground state. It would therefore be preferable that all the ions were in the ground state or, alternatively, that a possible metastable content could be shown not to influence the measured cross section.

In this experiment, the flight path from the stripping region to the gas cell is ~13 m. As the ions have velocities around v_0, the corresponding time of flight is of the order of 5×10^{-6} sec, which is considered to be longer than the lifetime of most metastable states of the emerging ions. We therefore expect the beam to contain only a small fraction of metastables, if any. However, to investigate experimentally the influence of a possible population of metastables in the beam, we used 20-MeV gold ($q=8$) ions created by stripping in the rest gas between the analyzing and the switching magnet, and compared the measured cross section with the result obtained with foil-stripped ions of the same charge. It is known[5] that these two methods to obtain highly charged ions may result in different populations of metastables, but we did not observe any significant difference in the measured cross sections.

However, this experimental check does not rule out that for specific charge states, the measured σ_C may be different from that obtained with ground-state ions. On the other hand, as the formation of metastables depends very much on the charge state of the ions, we expect that a possible content of metastables in the worst case could give rise to "bumps" in the cross section as a function of q but not influence the general dependence.

After a capture collision, the core of the $(q-1)$-charged ion might be excited, and if this excitation is large enough, autoionization may cause ejection of an electron. In case this process takes place prior to the subsequent charge analysis, the ion will not be registered as having made a capture, i.e., a lower capture cross section will be observed. For the highly charged ions used in this study, however, the capture cross section is probably much larger than the excitation cross sections; hence only a negligible part of the $(q-1)$-charged ions will autoionize. On the other hand, this has not been investigated experimentally, and a small influence from such effects on the measured cross sections cannot be ruled out.

In the case of double-electron capture, the effects of autoionization are probably more important, as the resulting ions emerge with at least two highly excited electrons. Therefore, we shall not present data for double-capture cross sections, although such data were in fact obtained; it suffices to state that generally, the observed double-capture cross sections were an order of magnitude smaller than the single-capture cross sections.

III. A SIMPLE THEORETICAL ESTIMATE

A number of theoretical investigations of electron capture have been made for medium- to high-velocity, highly charged ions colliding with atoms. However, due to the complexity of the three-body interaction capture process, it has been possible to perform *ab initio* calculations only for the simplest collision systems and only for limited ranges of the physical parameters involved. Hence, to acquire an understanding of the general dependence of the capture cross section on the experimental parameters, it is necessary to perform calculations based on simplified models. Here, we shall present such a calculation, from which we obtain general scaling laws as well as approximate quantitative results.

The calculation is based on a purely classical picture of the capture process. This is a reasonable approach, due to the high density of the final states which is found for highly charged ions, and also because the de Broglie wavelength of the projectile is much smaller than the collision diameter for the ion-target–electron interaction.

The model applies cross sections obtained by Bohr and Lindhard[4] for the capture from one-electron target atoms. They introduced two important ion-atom interaction distances in the following way. First, they argued that the electron can be released from the target nucleus when the projectile is close enough that the force excerted by it on the electron balances the binding force of the electron in the atom, i.e., when

$$qe^2/R_r^2 = mv^2/a\,, \tag{3}$$

where m, v, and a are the mass, velocity, and orbital radius of the electron, respectively. The so-called release distance R_r is thus given by

$$R_r = (qaa_0)^{1/2}(v_0/v)\,, \tag{4}$$

where $v_0 = e^2/\hbar$ is the first Bohr orbital velocity and $a_0 = \hbar^2/me^2$ is the corresponding orbital radius. Second, according to Bohr and Lindhard, the electron orbit will be polarized due to the strong ionic field during the approach of the ion so that at the moment of capture, the electron velocity will be greatly reduced with respect to the atom. Consequently, the condition for capture to take place is that the potential energy of the electron in the ionic field is numerically larger than its kinetic energy in the ion frame, i.e., the limiting condition for capture is given as

$$qe^2/R_c = \tfrac{1}{2}mV^2\,, \tag{5}$$

where V is the ion velocity, and hence capture is

possible when the ion-atom distance is smaller than

$$R_c = 2qa_0(v_0/V)^2 , \tag{6}$$

which is the so-called capture distance.

When $R_r < R_c$ and the ion is close enough for release to take place, the condition for capture is automatically fulfilled; hence, in this regime, the capture cross section is given by

$$\sigma_1 = \pi R_r^2 = \pi a_0^2 q (a/a_0)(v/v_0)^{-2} . \tag{7}$$

On the other hand, when $R_r > R_c$, release can take place before capture is possible, and if the release process happened instantaneously, the capture cross section would be zero. However, release is a gradual process, which takes place with a probability per unit time of the order of v/a, and as the time during which capture can occur is approximately R_c/V, the probability that a released electron will be captured is $(v/a)(R_c/V)$. Consequently, when $R_r > R_c$, the capture cross section is

$$\sigma_2 = \pi R_c^2 \left(\frac{v}{a}\frac{R_c}{V}\right) = 8\pi a_0^2 q^3 \left(\frac{a}{a_0}\right)^{-1}\left(\frac{v}{v_0}\right)\left(\frac{V}{v_0}\right)^{-7} . \tag{8}$$

From these results, we find that for low ion velocities and high ion charges, the cross section for capture from a one-electron atom is proportional to q and independent of the ion velocity V. On the other hand, for high-velocity ions, the cross section is proportional to q^3 and decreases with V^{-7}.

Having obtained cross sections for the capture of one electron, we now have to integrate over the electron distribution of the target atom. First, as the most simple possibility, we use a version of the Bohr statistical atomic model. The distribution of electrons dn as a function of velocity v is given by the atomic number z as

$$\frac{dn}{dv} = z^{1/3}\left(\frac{1}{v_0}\right), \tag{9}$$

whereas it is zero for v smaller than αv_a and larger than $\beta z v_0$, respectively. Here, v_a is given by the atomic ionization potential I via

$$v_a = v_0 (I/I_0)^{1/2} , \tag{10}$$

where $I_0 = \frac{1}{2}mv_0^2$. To be able to take into account the existence of electrons moving with velocities smaller than v_a, we introduce the adjustable parameter α, which therefore is expected to have a value between 0 and 1. For normalization reasons, the parameter β is given by

$$\beta = z^{-1/3} + \frac{\alpha}{z}\frac{v_a}{v_0} . \tag{11}$$

For heavy target atoms in this model, the highest electron velocity is therefore $z^{2/3}v_0$, which scales with z in the same way as the velocity in the more realistic statistical atomic models. The Bohr atomic model further assumes that the orbital radius and the velocity of the electrons are connected via

$$a = a_0 \frac{v_0}{v} z^{1/3} . \tag{12}$$

This equation is used to obtain the cross sections σ_1 for low-velocity [Eq. (7)] and σ_2 for high-velocity [Eq. (8)] ions, respectively, so that the target characteristics enter only via z and v:

$$\sigma_1 = \pi a_0^2 q z^{1/3} (v/v_0)^{-3} , \tag{13}$$

$$\sigma_2 = 8\pi a_0^2 q^3 z^{-1/3} (v/v_0)^2 (V/v_0)^{-7} . \tag{14}$$

Finally, these cross sections are integrated over the electron-velocity distribution, taking as a dividing velocity v_1 given by $\sigma_1 = \sigma_2$ or

$$v_1 = \left[\frac{z^{2/3}}{8q^2}\left(\frac{V}{v_0}\right)^7\right]^{1/5} v_0 . \tag{15}$$

It should be noted that v_1 is close to the ion velocity V.

Defining the parameter ξ as

$$\xi = q^{-2/7}(V/v_0) = (\tfrac{1}{25}E/q^{4/7})^{1/2} , \tag{16}$$

where E is the ion energy, (in keV/amu), the result of the integration can be written as

$$\frac{\sigma_C}{\pi a_0^2 q} = \begin{cases} \frac{1}{2}z^{2/3}\left[\left(\frac{\alpha v_a}{v_0}\right)^{-2} - (\beta z)^{-2}\right] & (v_1 < \alpha v_a) \\ \frac{8}{3}\xi^{-7}\left[\left(\frac{z^{2/3}}{8}\xi^7\right)^{3/5} - \left(\frac{\alpha v_a}{v_0}\right)^3\right] + \frac{1}{2}z^{2/3}\left[\left(\frac{z^{2/3}}{8}\xi^7\right)^{-2/5} - (\beta z)^{-2}\right] & (\alpha v_a < v_1 < \beta z v_0) \\ \frac{8}{3}\xi^{-7}\left[(\beta z)^3 - \left(\frac{\alpha v_a}{v_0}\right)^3\right] & (\beta z v_0 < v_1) . \end{cases} \tag{17}$$

This expression depends on the adjustable parameter α, but as shall be discussed later in this paper, for all but the lightest atoms, a value of 0.5 can be used. As it depends only on well-known parameters, Eq. (17) therefore suggests itself as a convenient first estimate of the capture cross section. For small ion velocities, the cross section is proportional to q and independent of V. Furthermore, for all but the lightest atoms, $\beta z \gg \alpha v_a/v_0$ so that $\sigma_C \propto z^{2/3} I^{-1}$ in this region. For large ion velocities, the cross section is proportional to q^3 and V^{-7}. Besides these dependences, an important aspect of the simple theoretical result is that it suggests the capture cross section for any target atom divided by the ion charge q to scale with the ion parameters in the combination $E(\text{keV/amu})q^{-4/7}$, a scaling which arises via the cross sections Eqs. (7) and (8), and therefore does not depend on the atomic model applied. The limits of applicability for Eq. (17) are given by the requirements that the ion charge should be high enough so the assumption that there is a quasi-continuum of states in the ion to which capture can take place is fulfilled, and that the ion velocity be small enough that quantal effects can be neglected in the description of the collision between the ion and the target electrons. These requirements lead to the criteria, for the first condition, for example, that $q \gtrsim 4$, and for the second, according to Bohr,[6]

$$2q(V/v_0)^{-1} \gg 1 . \tag{18}$$

IV. COMPARISON WITH EXPERIMENTAL DATA

Rather extensive experimental data exist for electron capture in collisions between highly charged ions ($q \geq 4$) and monatomic gases. In Figs. 3–6 is shown a comparison between such data and the theoretical estimate, Eq.(17). In each case, the adjustable parameter α has been found by fitting to the low-velocity data where σ_C is sensitive to changes in α. In the figures, the cross sections are plotted as $\sigma_C q^{-1}$ vs $E(\text{keV/amu})q^{-4/7}$, as suggested by Eq. (17).

Experimental data for an atomic hydrogen target are compared to Eq. (17) in Fig. 3. The data were obtained by Crandall *et al.*,[7] Phaneuf and Meyer,[8] Goffe *et al.*,[9] Kim *et al.*,[10] and Gardner *et al.*[11] (see the figure caption for details). From the figure it is seen that the data scale very well

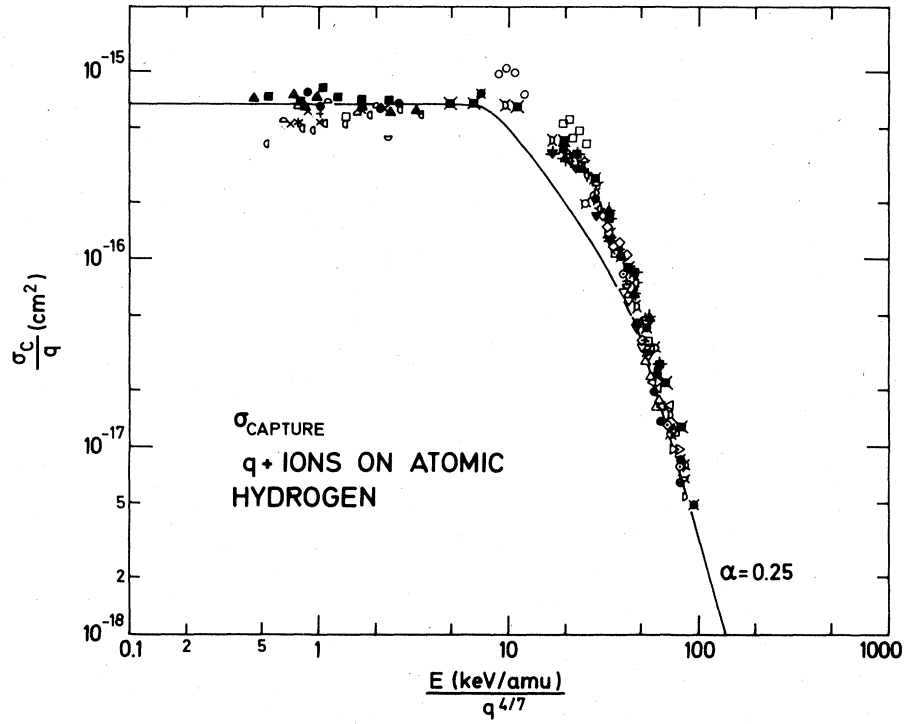

FIG. 3. Comparison between experimental data for the single-capture cross section for ions of charge $q \geq 4$ colliding with atomic H and the theoretical estimate [Eq. (17)]. The data were obtained by Crandall *et al.* (Ref. 7) (●: B^{4+}, ■:C^{4+}, ▲: N^{4+}, ▯ : B^{5+}, ▭: C^{5+}, ▭: N^{5+}, ▯ : O^{5+}, ×: O^{6+}, + : F^{6+}, *: Ar^{6+}), Phaneuf and Meyer (Ref. 8) (✱: C^{4+}, ✱ : N^{4+}, ✱: N^{5+}, ✱ : O^{4+}, ✱ : O^{5+}), Goffe *et al.* (Ref. 9) (✱ : B^{4+}, ✱: B^{5+}, ✱ : C^{4+}, ✱: C^{5+}, ✱ : C^{6+}), Kim *et al.* (Ref. 10) (⊙: Si^{5+}, ⊡ : Si^{6+}, ◈ : Si^{7+}), and Gardner *et al.* (Ref. 11) (○: Fe^{4-7+}, □ : Fe^{6-10+}, ◇ : Fe^{6-10+}, ▽: Fe^{7-11+}, △: Fe^{8-12+}, ◁:Fe^{9-13+}, ▷: Fe^{9-12+}).

when plotted as $\sigma_C q^{-1}$ vs $E(\text{keV/amu})q^{-4/7}$. The only points that deviate somewhat from the general trend of the data are the iron-ion measurements of Gardner *et al.* (○, □). However, it has been argued[7,12] that these results might be too large by as much as 50%. The absolute magnitude of the data deviate from the simple theoretical estimate for intermediate ion velocities. This is not surprising, as the distribution of electron velocities in the hydrogen atom is not well described by Eq. (9). A more realistic electron distribution might give a better agreement with the data. Nevertheless, there is an overall agreement within a factor of 2 between the simple estimate of Eq. (17) and the experimental data.

In Fig. 4, a similar comparison is shown for

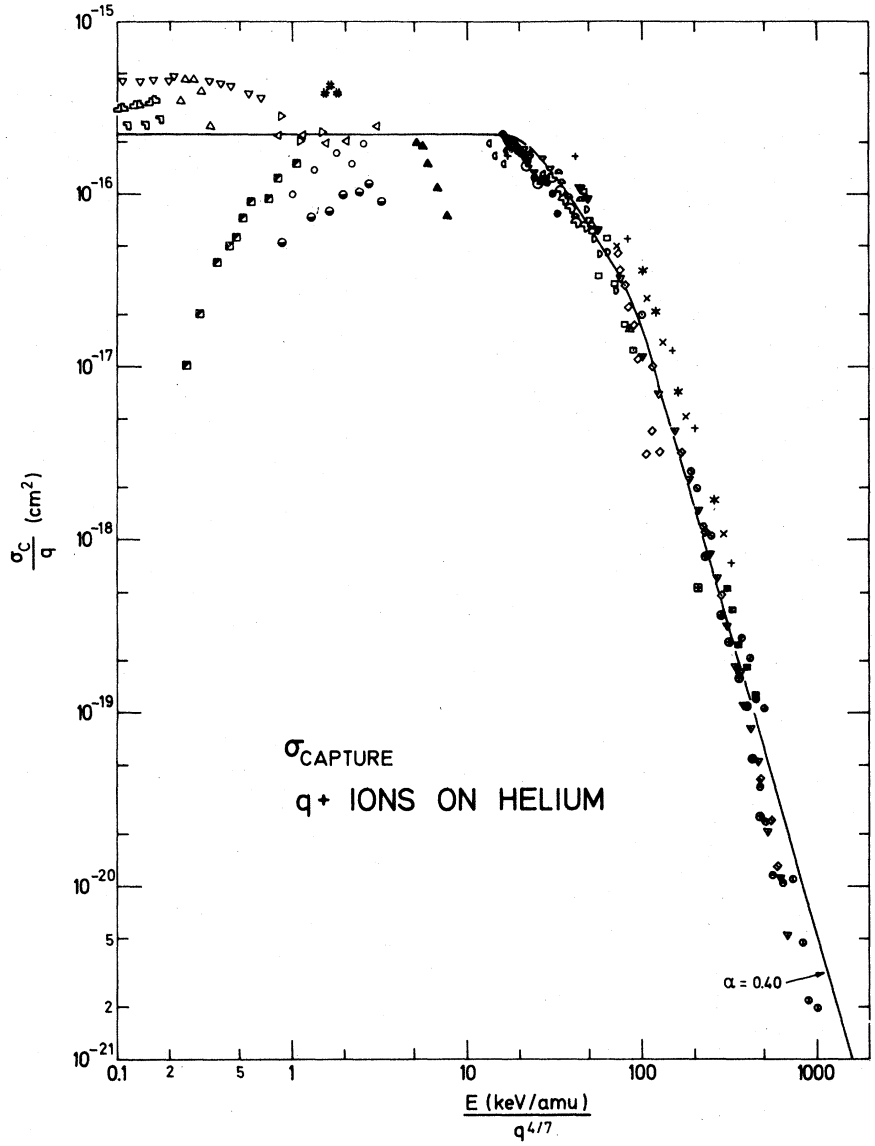

FIG. 4. Comparison between experimental data for the single-capture cross section for ions of charge $q \geq 4$ colliding with He atoms and the theoretical estimate [Eq. 17)]. The data were obtained by Zwally and Koopmann (Ref. 13) (▣: C^{4+}), Winter *et al.* (Ref. 14) (#: Ar^{6-8+}), Afrosimov *et al.* (Ref. 15) (◰: Ar^{5+}, ◱: Ar^{6+}, ◳: Ar^{7+}), Crandall (Ref. 16) (▷: O^{6+}, ◁: N^{5+}, ◒: C^{4+}), Macdonald and Martin (Ref. 17) (◐: O^{5-8+}, ⊖: O^{5-8+}, ⊘: O^{5-8+}, ⊗: O^{5-8+}), Müller and Salzborn (Ref. 18) (△: Ar^{4-8+}, ▽: Ar^{6+}), Moak *et al.* (Ref. 19) (⊞: I^{12+}), Datz *et al.* (Ref. 20) (□: Br^{4-10+}, ◇: Br^{5-13+}), Gardner *et al.* (Ref. 21) (○: B^{4+}), Nikolaev *et al.* (Ref. 22) (+: N^{4+}, ×: N^{5+}, *: N^{6+}), Guffey *et al.* (Ref. 23) (⊙: B^{5+}, ⊡: C^{6+}, ◬: N^{7+}, ▽: O^{8+}, ◈: F^{9+}), Schiebel *et al.* (Ref. 24) (⊕: Si^{14+}), and Betz *et al.* (Ref. 25) (◡: Br^{5-9+}, ◠: Br^{5-10+}, ◫: Br^{5-10+}, ▭: Br^{5-9+}, ◔: Br^{5-9+}, ◕: Br^{5-10+}). Furthermore, the data of this work are included (▲: Au^{4-8+}, ● : Au^{6-24+}, ▼: O^{4-6+}, ■ : O^{4-8+}).

helium as a target. The data were obtained by Zwally and Koopmann,[13] Winter *et al.*,[14] Afrosimov *et al.*,[15] Crandall,[16] Macdonald and Martin,[17] Müller and Salzborn,[18] Moak *et al.*,[19] Datz *et al.*,[20] Gardner *et al.*,[21] Nikolaev *et al.*,[22] Guffey *et al.*,[23] Schiebel *et al.*,[24] and Betz *et al.*[25] Also, the data of this work for $q \geq 4$, as presented in Fig. 2, are plotted in Fig. 4. From the figure it may be concluded that the scaling, as proposed by Eq. (17), works well for $E(\text{keV/amu})q^{-4/7} > 10$. For lower values of this parameter, large deviations are found. However, this may be attributed to the rather arbitrary definition of "highly charged" that has been used here, as the data deviating most from the calculated curve [by Zwally and Koopmann[13] (◩), Crandall[16] (⊖), and one of our data points (▲)] were measured with $q = 4$ ions. These data show a dependence on ion velocity which is normally found for cross sections for projectiles of low charge where, for fixed ion

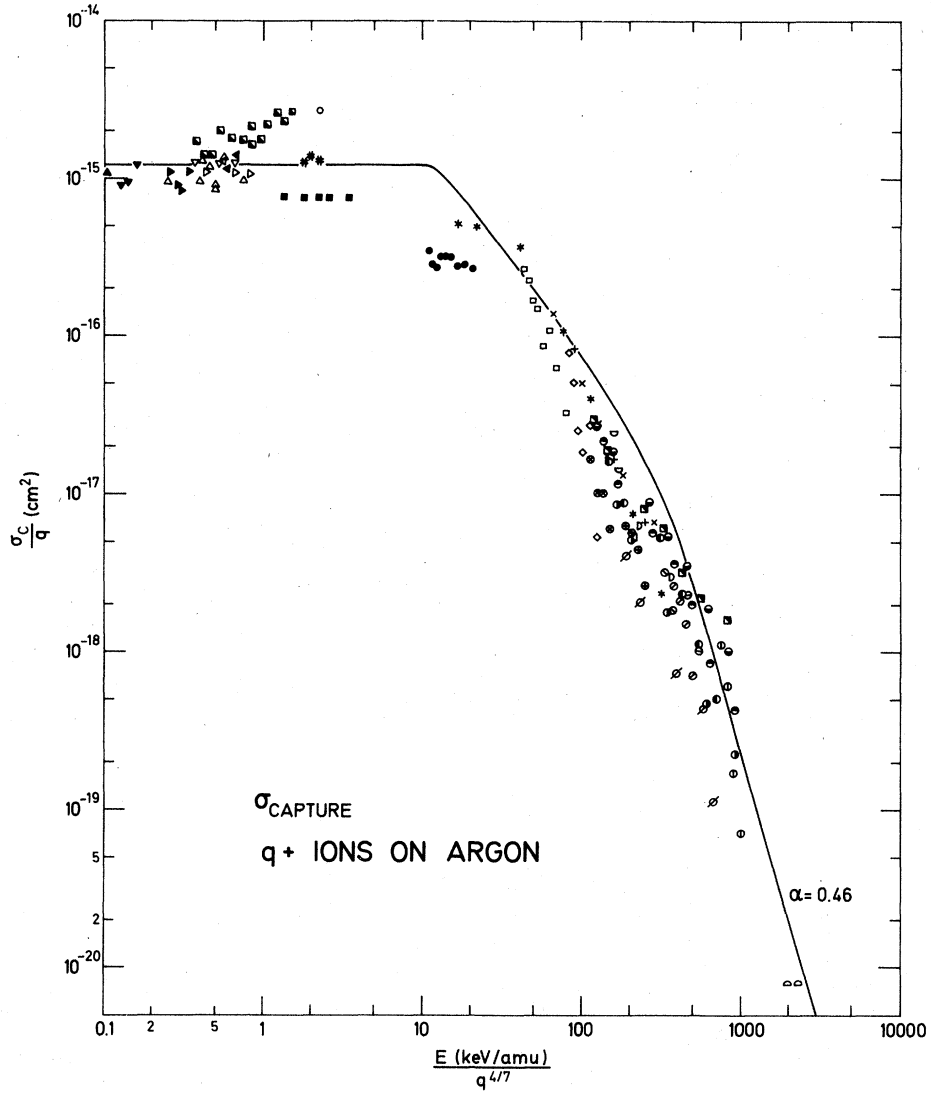

FIG. 5. A comparison between experimental data for the single-capture cross section for ions of charge $q \geq 4$ colliding with Ar atoms and the theoretical estimate [Eq. (17)]. The data were obtained by Gardner *et al.* (Ref. 21) (■: B^{4+}), Zwally and Koopman (Ref. 13) (◙: C^{4+}), Salzborn and Müller (Ref. 27) (▲: Xe^{4+}, ▼: Kr^{4-6+}, ▶: Ar^{4-7+}, ◀: Ne^{4-5+}), Macdonald and Martin (Ref. 17) (⊕: O^{5-8+}, ⊖: O^{5-8+}, ⊘: O^{5-8+}, ⊘: O^{5-8+}, ⊕: O^{5-8+}, ⊗: O^{5-8+}, only representative data are shown), Ferguson *et al.* (Ref. 28) (⊘: F^{4+}, ◑: F^{5+}, ◐: F^{6+} ⊖: F^{7+}, ◒: F^{8+}, ◙: F^{9+}, only representative data are shown), Klinger *et al.* (Ref. 29) (◁: Ar^{7+}, ▷: Ar^{6+}, △: Ar^{5+}, ▽: Ar^{4+}, ◬: Ar^{4-7+}), Winther *et al.* (Refs. 14 and 30) (○: Ne^{4+}, #: Ar^{4-6+}), Datz *et al.* (Ref. 20) (□: Br^{4-10+}, ◇: Br^{5-10+}), Nikolaev *et al.* (Ref. 22) (+: N^{6+}, ×: N^{5+}, *: N^{4+}), Moak (Ref. 31) (⊔: Br^{7-8+}), Moak *et al.* (Ref. 19) (⊏⊐: $Ar^{6,13+}$, ⊏: I^{12+}), Main (Ref. 32) (⊔: $Ar^{13,17+}$), and Meyer *et al.* (Ref. 12) (●: W^{4-12+}).

charge, the capture cross section decreases with decreasing ion velocity. Hence the breakdown of the scaling for low-velocity ions of low charge illustrates an expected limit of applicability for the simple estimate presented here. Disregarding data points obtained with low-velocity $q=4$ ions, the scaling is seen to be obeyed also in this case for helium as the target. Furthermore, with the same reservation, it is found that the absolute magnitude of the calculated curve agrees well with the data. A small deviation is found for the highest-velocity ions, where the experimental cross sections decrease more strongly with increasing velocity than does the V^{-7} dependence of Eq. (17). Once again, we reach a limit of applicability for the simple classical estimate, namely that given by Eq. (18). [For $q=4$, $2q(V/v_0)^{-1}=1$ when $E(\mathrm{keV/amu})q^{-4/7}=724$.] For combinations of q and V violating Eq. (18), we have to use quantal calculations like the one made by Brinkman and Kramers,[26] where the cross section is proportional to V^{-12}.

A more detailed comparison between the experimental results of this work and Eq. (17) is shown in Fig. 2, where the capture cross section is plotted as a function of ionic charge. Good agreement between the data and the theoretical result is observed with respect to absolute magnitude as well as dependence on q, except for low-charge, 3.3-MeV gold ions, where the theory is not strictly applicable.

Comparisons between Eq. (17) and experimental data for argon and krypton targets are shown in Figs. 5 and 6, respectively. In the case of argon targets, the data were obtained by Gardner *et al.*,[21] Zwally and Koopman,[13] Salzborn and

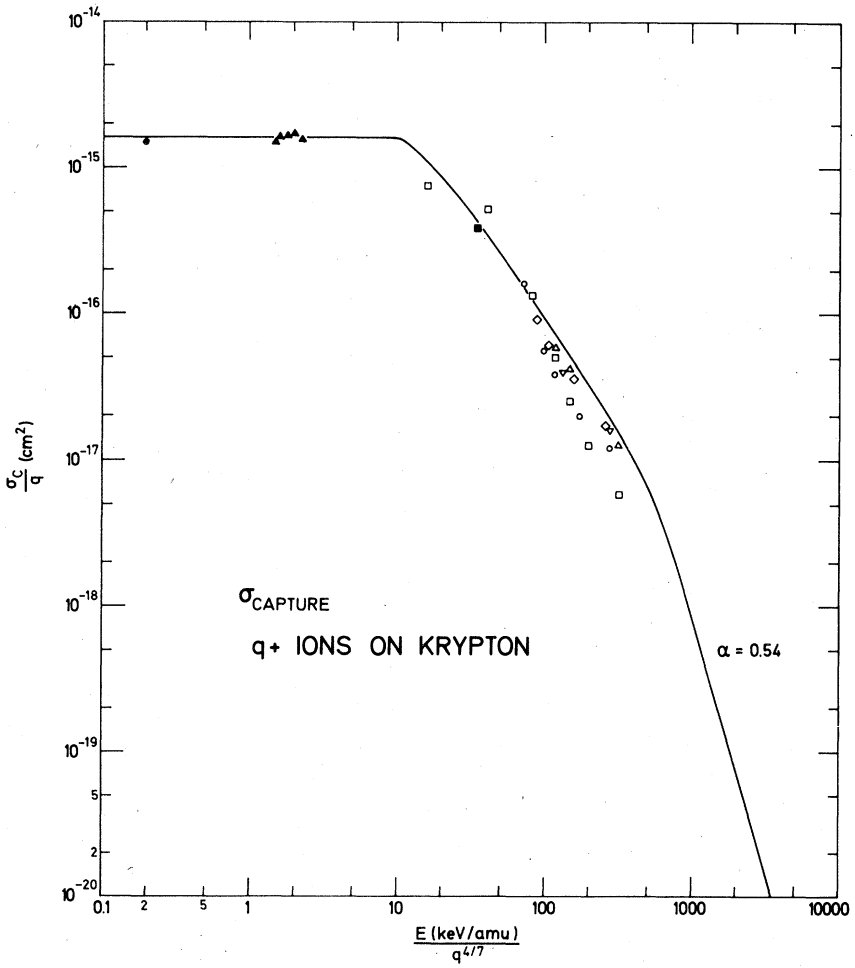

FIG. 6. A comparison between experimental data for the single-capture cross section for ions of charge $q \geq 4$ colliding with Kr atoms and the theoretical estimate [Eq. (17)]. The data were obtained by Winter *et al.* (Ref. 14) (▲: Ar^{4-8+}), Betz (Ref. 33) (■: Ar^{5+}), Müller *et al.* (Ref. 34) (●: Xe^{10+}), and Nikolaev *et al.* (Ref. 22) (△: B^{4+}, ▽: B^{5+}, □: N^{4+}, ○: N^{5+}, ◇: N^{6+}).

Müller,[27] Macdonald and Martin,[17] Ferguson *et al.*,[28] Klinger *et al.*,[29] Winter *et al.*,[14,30] Datz *et al.*,[20] Nikolaev *et al.*,[22] Moak,[31] Moak *et al.*,[19] Main,[32] and Meyer *et al.*[12] The krypton data were obtained by Winter *et al.*,[14] Betz,[33] Müller *et al.*,[34] and Nikolaev *et al.*[22]

The scaling in Figs. 5 and 6 again is rather satisfactory. However, there are two sets of data deviating from the general trend of the other experimental results, namely the argon-target data of Zwally and Koopmann (◪) and Meyer *et al.* (●). It has been suggested[16] that the measurements of Zwally and Koopmann are a factor of ~3 too high due to experimental difficulties. Furthermore, the data of Meyer *et al.* were obtained with the very heavy projectile tungsten, and, as will be discussed later, there may be a special mechanism that leads to small cross sections in this case. Consequently, the scaling of $\sigma_C q^{-1}$ vs $E(\mathrm{keV/amu})q^{-4/7}$ is likely to be valid for argon and krypton targets as well.

With respect to the absolute magnitude of the results of Eq. (17), an overall agreement with the experimental data is found, except at the positions where the calculated curve "kinks". This behavior is due to the crude electron-velocity distribution applied, and it would probably be more satisfactory if a more realistic atomic model were used. For example, near $E(\mathrm{keV/amu})q^{-4/7}=200$, there is a shoulder in the general trend of the data of Fig. 5. This stems from the shell structure of the argon atom. Calculations by Janev *et al.*,[35] using the Brinkman-Kramers formalism, show the shoulder to arise because above $E(\mathrm{keV/amu})q^{-4/7}=200$, electrons in the argon L shell can be captured, and this yields an increased total cross section.

Generally, it can be concluded that Eq. (17) gives a good first estimate of the absolute magnitude of the single-capture cross section for highly charged, medium or high-velocity ions colliding with any atom.

In a detailed comparison with experimental data, however, we may encounter a number of small deviations from Eq. (17), some of which have already been mentioned. Due to the crude electron distribution used in obtaining Eq. (17), the theoretical result shows kinks and does not reproduce the detailed behavior due to shell effects like that seen in Fig. 5. Furthermore, the theory presented here is valid for pointlike, highly charged ions and hence does not take into account effects stemming from the structure of the ions. We have already mentioned that at low ion velocity, there are deviations due to the influence from the detailed electron structure for relatively low-charged ions. Further, Eq. (17) does not show "dips" for the cross section for ions having closed shells, as observed by, e.g., Meyer *et al.*,[12] and it does not reproduce the oscillatory behavior as a function of q, as also observed by Meyer *et al.*,[12] for H, H_2, and Ar targets for very heavy ions. This effect is considered to be due to interference between the long-range and the short-range-screened Coulomb potentials of the heavy ions. An example of such data obtained on an atomic-hydrogen target with tantalum ions is shown in Fig. 7, once again plotted in reduced variables, and compared to Eq. (17). We observe that the theoretical curve reproduces the overall trend even of these oscillatory data. Also, as can be concluded via a comparison with Fig. 3, the interference effect seems to cause a decrease of the cross section relative to that for ideal, highly charged ions. Meyer *et al.* found the amplitude of these oscillations to decrease with increasing target-electron binding energy. Hence it is consistent with their findings that our data obtained with a comparable ion velocity (20-MeV gold ions) show very little, if any, oscillation; the electron-binding energy of helium being much larger than those for H, H_2, and Ar.

With respect to the scaling suggested by Eq. (17), this is fulfilled rather accurately for the experimental data presented in Figs. 3–6. As mentioned previously, this scaling is independent of the atomic model used to describe the target atom in the calculations and is considered to be universal.

Equation (17) contains the adjustable parameter α, which was introduced to determine the lowest effective electron velocity αv_a of the target atom. Physically, it describes the fact that there exist electrons moving with a lower velocity than v_a, corresponding to the ionization potential via Eq. (10). The parameter α can be found for each target atom by fitting to low-velocity–high-charge ion data. The values obtained for H, He, Ar, and Kr-target data of Figs. 3–6 are shown in Fig. 8. To investigate further the dependence of α on the target atomic number, we used the 200-keV argon-ion ($q=5$–8) data for He, Ne, Ar, Kr, and Xe of Winter *et al.*[14] and the 100-keV xenon-ion ($q=10$) data for He, Ne, Na, Ar, Kr, Cd, Xe, and Cs targets of Müller *et al.*[34] The values of α obtained from these data are also shown in Fig. 8. It can be seen that for not too light target atoms, which are expected to be fairly well described by statistical atomic models such as the Bohr model, a value of $\alpha=0.5$ gives a good fit to the experimental data both for targets of high ionization potentials (Ne, Ar, Kr) and for those with low ionization potentials (Cs, Cd). One exception is the result obtained from the sodium-data point of

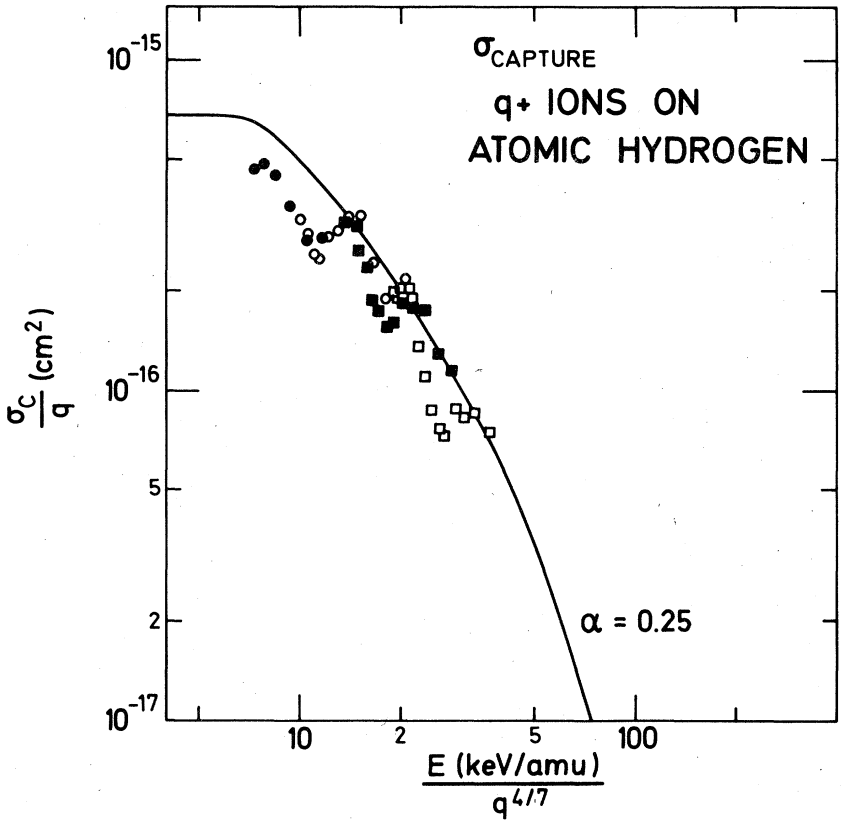

FIG. 7. A comparison between experimental data of Meyer *et al.* (Ref. 12) and Eq. (17). The data were obtained with Ta ions with ●: $q=4-9$, ○: $q=4-14$, ■: $q=5-18$, and □: $q=6-19$.

Müller *et al.*, but further data are needed to check whether this deviation is real or not. For the light targets (H, He), values of α smaller than 0.5 are obtained, which is not surprising, as these atoms are not well described by simple statistical models. However, for all target atoms, Fig. 8 gives the basis for obtaining the proper value of α to be used in Eq. (17).

Based on the information of Fig. 8, it seems justified to assume that α is approximately independent of the target atomic number for all but the lightest target atoms. Consequently, from Eq. (17) we find that for low-velocity, highly charged ions,

$$\sigma_C \propto q z^{2/3} I^{-1} . \tag{19}$$

The dependence of σ_C on the target-ionization potential has been discussed by Salzborn and Müller,[27] who fitted a large number of experimental data for target atoms having $I \geq 12$ eV to the expression

$$\sigma_C \propto q^{\alpha} I^{\beta} \tag{20}$$

and found $\alpha = 1.17$ and $\beta = -2.76$. However, when taking into account data for target atoms with small ionization potentials, they had to change the value of β to -1.94. From a plot of I for the noble gases as a function of atomic number, it can be found that it is approximately proportional to $z^{-1/3}$. Using this dependence in Eq. (19), we find $\sigma_C \propto I^{-3}$, which is close to the empirical results of Salzborn and Müller. However, Eq. (19)

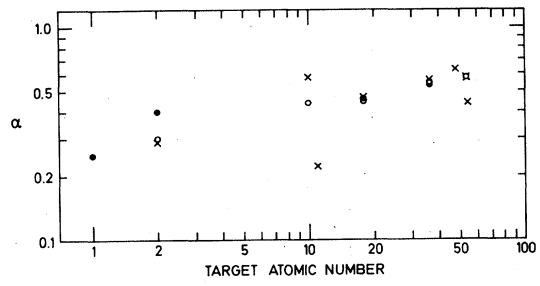

FIG. 8. The adjustable parameter α as found by fitting Eq. (17) to experimental data obtained with low-energy, highly charged ions. The values of α were obtained from ●: The low-energy data of Figs. 3–6, ○: 200-keV Ar ions with $q=5-8$ from Winter *et al.* (Ref. 14), and ×: 100-keV Xe^{10+} data of Müller *et al.* (Ref. 34).

suggests that a better empirical fit to the data can be obtained if instead of Eq. (20), the data are fitted to $q^{\alpha}z^{\gamma}I^{\beta}$, i.e., including the target atomic number as a variable.

V. CALCULATION BASED ON THE LENZ-JENSEN ATOMIC MODEL

In Sec. III, we derived a simple estimate of the electron-capture cross section [Eq. (17)] using the Bohr-Lindhard cross sections [(Eqs. (7) and (8)] for the capture of one "classical" electron combined with the statistical Bohr atom-electron distribution [Eq. (9)]. It was found that the simple estimate leads to general rules for scaling with projectile parameters q and V as well as to quantitative approximate results. However, it is clear that it is interesting to apply a more realistic model for describing the target-atom electron distribution. Here we have used the statistical first-order Lenz-Jensen atomic model,[36] which rather accurately describes the overall dependence of the density of electrons ρ as a function of distance a from the target-atom nucleus. Introducing the reduced distance

$$x=(a\lambda/a_0)^{1/2}z^{1/6}, \tag{21}$$

where $\lambda=10.91$, the spatial density of electrons is given by

$$\rho(x)=\frac{z}{A}\frac{e^{-x}}{x^3}(1+C_1x)^3, \tag{22}$$

where $A=4\pi a_0^3\lambda^{-3}z^{-1}P$, $P=28.118$, and $C_1=0.265$. Combining this result with the Bohr-Lindhard cross sections, we can find the capture cross section from

$$\sigma_C=\int_0^{x_1}\sigma_1(x)\rho(x)dx+\int_{x_1}^{\infty}\sigma_2(x)\rho(x)dx, \tag{23}$$

where $\sigma_1(x)$ and $\sigma_2(x)$ are expressed as functions of x. From Eqs. (7) and (8) it can be seen that such expressions can be found via a knowledge of the mean electron velocity as a function of x. To this end, we use that for an electron gas in the ground state, the maximum electron velocity is the Fermi velocity,

$$v_F=\frac{\hbar}{m}(3\pi^2\rho)^{1/3}. \tag{24}$$

Using the well known density of electrons in phase space, we find $v=\frac{3}{4}v_F$; hence we can find $v(x)=\frac{3}{4}v_F(x)$ by combining Eqs. (22) and (24). The integration limit x_1 is equivalent to v_1 used in Sec. III, i.e., it is given via the equation $\sigma_1(x_1)=\sigma_2(x_1)$, which leads to the expression

$$e^{x_1}x_1^7(1+0.265x_1)^{-3}=43\,714\,\Xi^{-7}, \tag{25}$$

where the parameter Ξ is defined as

$$\Xi=q^{-2/7}z^{-8/21}(V/v_0). \tag{26}$$

Finally, from Eq. (23), we find

$$\frac{\sigma_C z^{2/3}}{\pi a_0^2 q}=\begin{cases}5.085\times10^{-4}\displaystyle\int_0^{x_1}e^{-x/3}x^6(1+0.265x)dx\\ +22.23\Xi^{-7}\displaystyle\int_{x_1}^{\infty}e^{-4x/3}x^{-1}(1+0.265x)^4dx.\end{cases} \tag{27}$$

According to Eq. (25), x_1 depends on Ξ only; hence this is true also for the right-hand side of Eq. (27). Consequently, we are led to a universal scaling, valid for any atom which is properly described by the Lenz-Jensen model, namely that for highly charged ions, the reduced capture cross section $\sigma_C z^{2/3}q^{-1}$ depends on the parameter Ξ only or, alternatively, on the value of the expression $E(\mathrm{keV/amu})q^{-4/7}z^{-16/21}$.

In Fig. 9, the result of this calculation is compared to cross sections obtained from Eq. (17), which we know from Sec. IV to be close to the experimental results. As can be seen, the Lenz-Jensen result agrees with the other curves, and thus with experiment, for not too low values of Ξ. For low Ξ values, the experimental cross sections deviate from the Lenz-Jensen result, but the deviation occurs for lower Ξ values, the lower the target-ionization potential. To a certain extent, the Lenz-Jensen cross section is the limit of the real cross sections in the respect that the experimental results all coincide with the Lenz-Jensen cross section for large Ξ, and so that a hypothetical target atom with zero ionization potential containing very many electrons would have a cross section equal to the Lenz-Jensen result.

VI. OTHER THEORETICAL CALCULATIONS

There exist a number of theoretical calculations of the electron-capture cross section for highly charged ions of medium or high energies. For reference, see, e.g., Ref. 37. As the main emphasis of this work has been on scaling properties, two of the works which also suggest scaling laws should be mentioned; for atomic hydrogen targets, Ryufuku and Watanabe[38] used a so-called unitarized, distorted-wave approximation to calculate the electron-capture cross section for a number of fully stripped ions. Their results are shown in Fig. 10, compared to the simple esti-

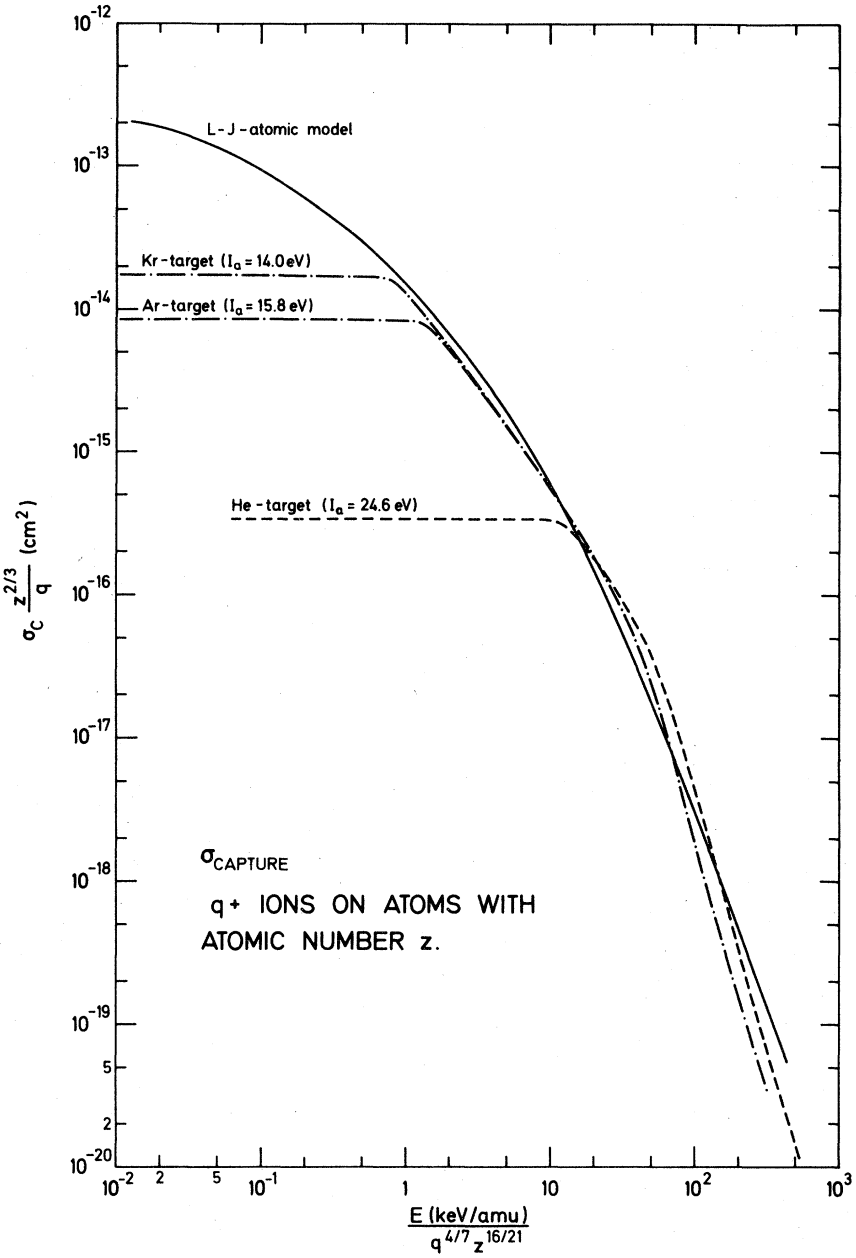

FIG. 9. The electron-capture cross section found from Eq. (27), which is based on the Bohr-Lindhard cross sections and the Lenz-Jensen atomic model. It is compared to the results for He, Ar, and Kr targets obtained from the simple estimate [Eq. (17)].

mate [Eq. (17)] and plotted using the scaling inherent in that equation. As can be seen, their medium- and high-energy results scale perfectly with $E(\text{keV/amu})q^{-4/7}$, adding further credibility to the ion-parameter scaling suggested in the present work. Ryufuku and Watanabe suggested a scaling with q and V for atomic hydrogen targets. They plotted their results as $\sigma_C q^{-1.12}$ vs $E(\text{keV/amu})q^{-0.45}$. Here the power -1.12 was found by simple fitting to the calculated results, whereas the reduced energy was found by dividing the ion energy with the hydrogenlike energy of the level most likely populated by the captured electron. As they found the most populated quantum level to vary as $\bar{n} \propto q^{0.774}$, and as the energy of hydrogenlike states in the ion varies as $q^2 n^{-2}$, they normalized the ion energy with $q^{0.45}$. This scaling is very close to that suggested in the present work to be valid for all target atoms.

Recently, Janev *et al.*[35] published calculations

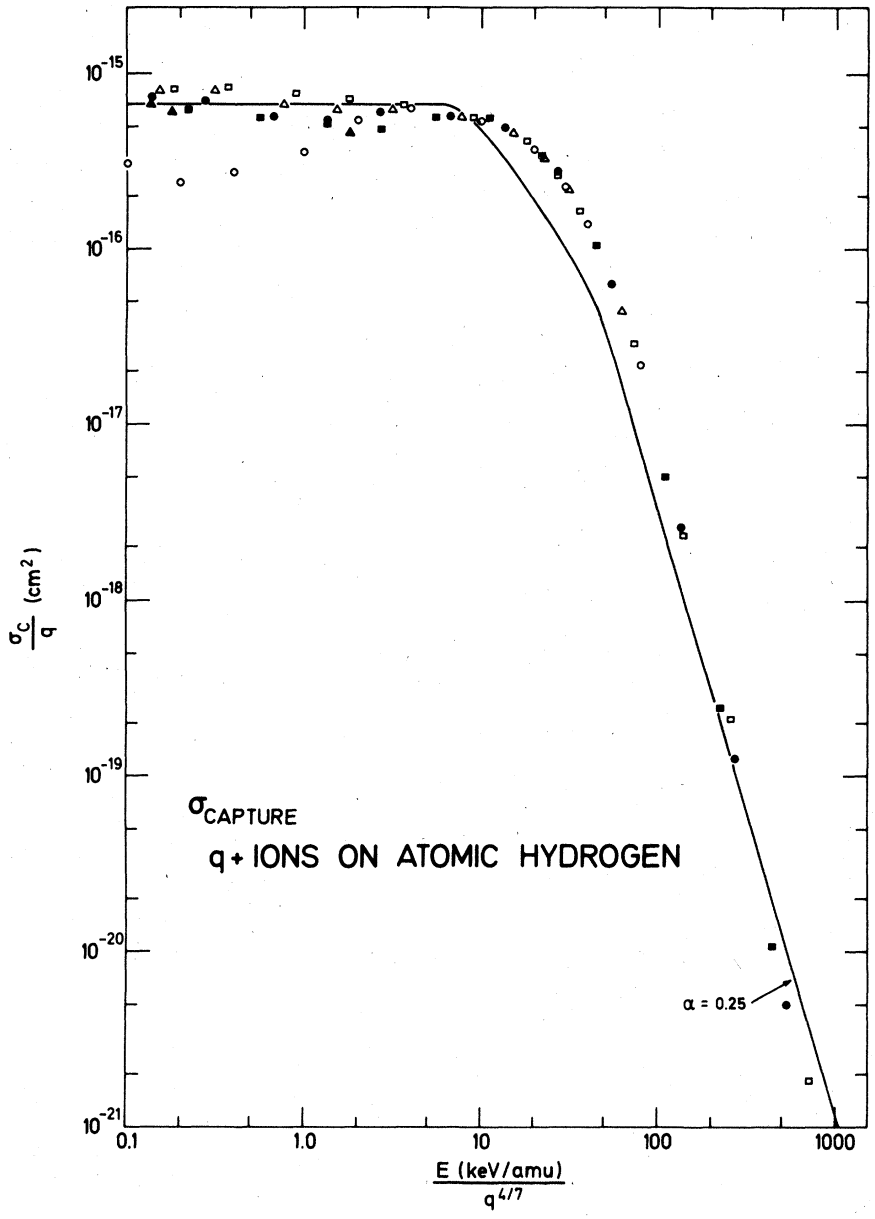

FIG. 10. Calculations for bare ions on atomic H targets by Ryufuku and Watanabe (Ref. 38) based on the unitarized distorted-wave approximation. Their results (○: $q=5$, □: $q=6$, △: $q=8$, ●: $q=10$, ■: $q=14$, and ▲: $q=20$) are plotted according to the scaling suggested in this work and compared to Eq. (17).

for highly charged ions colliding with argon atoms. They used the first Born approximation to calculate the partial cross sections for capture from the individual argon atomic-electron shells and obtained the total cross section as the sum of the partial values. They used a scaling where $\sigma_C q^{-2}$ was plotted versus $E(\text{keV/amu})q^{-1/2}$ and noted that the reduced energy parameter has the meaning of the ion energy divided by the binding energy of the captured electron in the populated ionic level. While the scaling of the ion energy suggested by Janev *et al.* agrees with those suggested by Ryufuku and Watanabe and by us, their cross-section scaling ($\sigma_C q^{-2}$) is at variance with those suggested in Ref. 38 ($\sigma_C q^{-1.12}$) and in this work ($\sigma_C q^{-1}$).

[1]G. H. Henderson, Proc. R. Soc. London A102, 496 (1922).
[2]See, e.g., H. W. Drawin, Phys. Rep. 37, 125 (1978).
[3]See, e.g., G. Steigman, Astrophys. J. 199, 642 (1975).
[4]N. Bohr and J. Lindhard, K. Dan. Vidensk. Selsk. Mat. Fys. Medd. 28, No. 7 (1954).
[5]V. S. Nikolaev, I. S. Dimitriev, Yu. A. Tasheev, Ya. A. Teplova, and Yu. A. Fainberg, J. Phys. B 8, L58 (1975).
[6]N. Bohr, K. Dan. Vidensk. Selsk. Mat. Fys. Medd. 18, No. 8 (1948).
[7]D. H. Crandall, R. A. Phaneuf, and F. W. Meyer, Phys. Rev. A 19, 508 (1979).
[8]R. A. Phaneuf and F. W. Meyer, Phys. Rev. A 17, 538 (1978).
[9]T. V. Goffe, M. B. Shah, and H. B. Gilbody, J. Phys. B 12, 3763 (1979).
[10]H. J. Kim, R. A. Phaneuf, F. W. Meyer, and P. H. Stelson, Phys. Rev. A 17, 854 (1978).
[11]L. D. Gardner, J. E. Bayfield, P. M. Koch, H. J. Kim, and P. H. Stelson, Phys. Rev. A 16, 1415 (1977).
[12]F. W. Meyer, R. A. Phaneuf, H. J. Kim, P. Hvelplund, and P. H. Stelson, Phys. Rev. A 19, 515 (1979).
[13]H. Jay Zwally and D. W. Koopmann, Phys. Rev. A 2, 1851 (1970).
[14]H. Winter, Th.M. El-Sherbini, E. Bloemen, F. J. de Heer, and A. Salop, Phys. Lett. 68A, 211 (1978).
[15]V. V. Afrosimov, A. A. Basalaev, M. N. Panov, and G. A. Leiko, Pis'ma Zh. Teor. Fiz. 26, 699 (1977) [JETP Lett. 26, 537 (1977)].
[16]D. H. Crandall, Phys. Rev. A 16, 958 (1977).
[17]J. R. Macdonald and F. W. Martin, Phys. Rev. A 4, 1965 (1971).
[18]A. Müller and E. Salzborn, Phys. Lett. 59A, 19 (1976).
[19]C. D. Moak, H. O. Lutz, L. B. Bridwell, L. C. Northcliffe, and S. Datz, Phys. Rev. 176, 427 (1968).
[20]S. Datz, H. O. Lutz, L. B. Bridwell, C. D. Moak, H. D. Betz, and L. D. Ellsworth, Phys. Rev. A 2, 430 (1970).
[21]L. D. Gardner, J. E. Bayfield, P. M. Koch, I. A. Sellin, D. J. Pegg, R. S. Peterson, M. L. Mallory, and D. H. Crandall, Phys. Rev. A 20, 766 (1979).
[22]V. S. Nikolaev, I. S. Dimitriev, L. N. Fateeva, and Ya. A. Teplova, Pis'ma Zh. Eksp. Teor. Fiz. 40, 989 (1961) [JETP Lett. 13, 695 (1961)].
[23]J. A. Guffey, L. D. Ellsworth, and J. R. Macdonald, Phys. Rev. A 15, 1863 (1977).
[24]U. Schiebel, B. L. Doyle, J. R. Macdonald, and L. D. Ellsworth, Phys. Rev. A 16, 1089 (1977).
[25]H. D. Betz, G. Ryding, and A. B. Wittkower, Phys. Rev. A 3, 197 (1971).
[26]H. C. Brinkman and H. A. Kramers, Proc. Acad. Sci. Amsterdam 33, 973 (1930).
[27]E. Salzborn and A. Müller, *Invited Lectures of the XI ICPEAC, Kyoto, 1979*, edited by K. Takayanagi and N. Oda (The Society for Atomic Collisional Research, Kyoto, 1979), p. 407.
[28]S. M. Ferguson, J. R. Macdonald, T. Chiao, L. D. Ellsworth, and S. A. Savoy, Phys. Rev. A 8, 2417 (1973).
[29]H. Klinger, A. Müller, and E. Salzborn, J. Phys. B 8, 230 (1975).
[30]H. Winter, E. Bloemen, and F. J. de Heer, J. Phys. B 10, L453 (1977).
[31]C. D. Moak (private communication), see Ref. 33.
[32]B. Main private communication, see Ref. 33.
[33]H. D. Betz, Rev. Mod. Phys. 44, 465 (1972).
[34]A. Müller, C. Achenbach, and E. Salzborn, Phys. Lett. 70A, 410 (1979).
[35]R. K. Janev, L. P. Presnyakov, and V. P. Shevelko, Phys. Lett. 76A, 121 (1980).
[36]See, e.g., P. Gombas, *Die Statistische Theorie des Atoms und ihre Anwendungen* (Springer, Vienna, 1949), p. 72.
[37]R. K. Janev and L. P. Presnyakov, Phys. Rep. (in press).
[38]H. Ryufuku and T. Watanabe, Phys. Rev. A 18, 2005 (1978); 19, 1538 (1979); 20, 1828 (1979).